Effect of Iron Doping on Physical Properties of NiO Thin Films

O. Belahssen[1,2,*], M. Ghougali[1,2,3], A. Chala[1,2]

[1] *Material Sciences Department, Faculty of Science, University of Biskra, Algeria*
[2] *Physic Laboratory of Thin Films and Applications (LPCMA), University of Biskra, Algeria*
[3] *Laboratory of exploitation and valorization the azalea energetics sources (LEVRES), Faculty of exact Science, University of El-Oued, Algeria*

Nickel-iron oxide was deposited on highly cleaned glass substrates using spray pneumatic technique. The effect of iron percentage on structural, optical and electrical properties has been studied. The crystalline size of the deposited thin films was calculated using Debye-Scherer formula and found in the range between 8.8 and 27.6 nm. The optical properties have been discussed in this work. The absorbance (A), the transmittance (T) and the reflectance (R) were measured and calculated. Band gap energy is considered one of the most important optical parameter, therefore measured and found ranging between 3.81 and 3.98 eV. The NiO:Fe thin film reduces the light reflection for visible range light. The increase of the electrical conductivity to maximum value of $0.470\ 10^{-4}\ (\Omega\ cm)^{-1}$ for 6 % Fe can be explained by the increase in carrier concentration of the films. A good electrical conductivity of the NiO:Fe thin film is obtained due to the electrically low sheet resistance. NiO:Fe can be applied in different electronic and optoelectronic applications due to its high band gap, high transparency and good electrical conductivity.

Keywords: NiO thin films, XRD, Optical constants, Electrical conductivity.

1. INTRODUCTION

Nickel oxide (NiO) is the most investigated metal oxide and it has attracted considerable attention because of its low cost material, and also for its applications in several fields such as a catalyst, transparent conducting oxide, photodetectors, electrochromic, gas sensors, photovoltaic devices, electrochemical supercapacitors, heat reflectors, photo-electrochemical cell, solar cells and many opto- electronic devices [1-9]. NiO is an IV group and it can be used as a transparent p-type semiconductor layers, it has a band gap energy ranging from 3.45 eV to 3.85 eV [10]. Band gap energy is significant to adjust the energy level state of NiO.

Several techniques have been used for synthesis and manipulation of nanostructures NiO:Fe such as the thermal evaporation, sputtering, pulse laser ablation, thermal decomposition, electrochemical deposition and sol–gel methods etc. Among of these techniques, sol-gel has some advantages such as high purity of raw materials and a homogeneous solution hence easy control over

In this work, a low cost spray pneumatic technique was used to prepare pure NiO:Fe nanoparticles thin films with various iron percentages. The structural properties of the produced nickel oxide doped iron thin films have been examined. The absorption, transmittance and reflectance spectra of the produced thin films for the NiO:Fe are also measured in range between 300-1100 nm. Moreover, the optical band gap is determined as a function of the iron percentages.

2. EXPERIMENTAL DETAILS

2.1 Preparation of Samples

NiO:Fe thin films were prepared onto a highly cleaned glass substrates using spay pneumatic technique. Nickel nitrate was dissolved in 50 ml of water as a solvent, iron nitrate was dissolved in 50 ml of water too and chloride acid was used as a stabilizer for the all samples in this work. The precursor molarity and iron nitrate concentration are 0.20 mol L^{-1}. The produced mixture was stirred at 60 °C for 2 h in order to obtain a clear and homogenous solution then the mixture was cooled down at room temperature and placed at dark environment for 48 h. The glass substrates were cleaned by detergent and by alcohol mixed with deionized water.

2.2 Deposition of Thin Films

The coating was dropped into glass substrates at 480 °C that sprayed during 2 min by pneumatic nebulizer system which transforms the liquid to a stream formed with uniform and fine droplets.

2.3 Devices and Measurements

The X-ray diffraction (XRD) spectra of the NiO:Fe were measured to verify the structure. X-ray diffraction (XRD) was measured by using BRUKER-AXS-8D diffractometer with Cu Kα radiation ($\lambda = 1, 5406$ Å) operated at 40 kV and 40 mA in the scanning range of (2θ) between 20° and 80°. The spectral dependence of the NiO:Fe transmittance (T) and the absorbance (A), on the wavelength ranging 300-1100 nm are measured using an ultraviolet-visible spectrophotometer (Perkin-Elmer Lambda 25). The reflectance (R) was calculated by the well-known equation as ($T + R + A = 1$). Whereas the electrical conductivity of the films was measured in a coplanar structure of four golden stripes on the deposited film surface; the measurements were performed with Keithley model 2400 low voltage source meter instrument.

* belahssenokba@gmai.com

3. RESULTS AND DISCUSSIONS

3.1 Structural Properties

The X-ray diffraction was used in this work in order to understand the structure of the deposited NiO:Fe thin films with different iron percentages. XRD patterns of all the deposited samples of Nickel-Iron Oxide thin films are shown in figure 1. From the figure, it can be noticed that all the patterns exhibit diffraction peaks around $2\theta \sim 37°$, referred to (111) favorite direction which is in agreement with the Joint Committee of Powder Diffraction Standards (JCPDS) card number 47-1049. The position of the peaks leads to the conclusion that the films are, in nature, with a cubic crystalline structure, which is in agreement with other reports [11, 12].
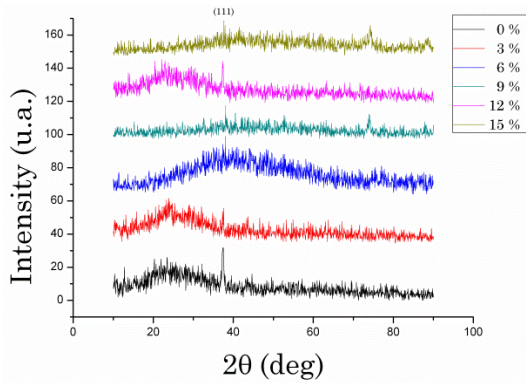

Fig. 1 – XRD patterns of the deposited NiO:Fe thin films on glass substrate at different iron percentages

The lattice constant a of Fe doped NiO thin films, is calculated using equation (1):

$$d_{(hkl)} = \frac{a}{\sqrt{\left(h^2 + k^2 + l^2\right)}}, \qquad (1)$$

where (h, k, l) is the Miller indices of the planes and d_{hkl} is the interplanar spacing.

It can be observed that no peaks correspond to the Fe doping exist in the XRD patterns. In fact, doping with low concentration impurities does not result in the appearance of new XRD peaks, but instead leads to a shift in the lattice parameters of the host material. This shift may arise from the strain induced when the dopant is incorporated into the crystal lattice [13]. The strain ε values in the films were estimated from the observed shift, in the diffraction peak between their positions in the XRD spectra via the formula (2):

$$\varepsilon = \frac{a - a_0}{a_0} \cdot 100 \qquad (2)$$

where ε is the mean strain in NiO:Fe thin films (Table 1), a is the lattice constant of NiO:Fe thin films and a_0 the lattice constant of bulk (standard $a_0 = 0, 4177$ nm).

The crystalline size was calculated using Debye-Scherer formula [14]:

$$D = \frac{0.9\lambda}{\beta \cos \theta} \qquad (3)$$

where β is the full width at half maximum (FWHM) and θ is the diffraction angle.

The crystallite size of the NiO:Fe thin films were calculated using the well-known Deby-Scherer's formula Eq. (3), the average of the NiO:Fe thin films ranging between 8.8 and 27.6 nm. The changing in the crystallites size leads to the changes in optical properties.

Fig. 2 shows the variation of the crystallite size and mean strain as a function of percentage of Fe. The crystallite size increases when the stain decreases and inversely.

The changing in the crystallites size leads to the changes in optical properties i.e. band gap energy increases with decreasing crystallites size as shown in Fig. 3.
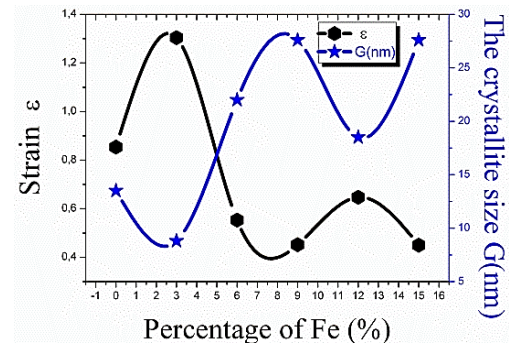

Fig. 2 – The variation of crystallite size and mean strain of Fe doped NiO thin films as a function of the percentage of Fe
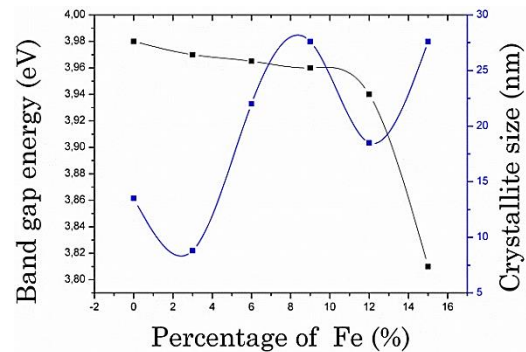

Fig. 3 – The variation of crystallite size and band gap energy of NiO:Fe thin films as a function of the percentage of Fe

3.2 Optical Properties

Fig. 4 shows the optical absorption spectra of NiO:Fe nanoparticles. The absorption spectra of 6 % Fe show that the absorption edge is slightly shifted towards shorter wavelength when compared to other absorption spectra. The absorption edge of a degenerate semiconductor is shifted to shorter wavelengths with increasing carrier concentration. This shift predicts that there is an increase in band gap value ($E_g = 3.965$ eV). The fundamental absorption, which corresponds to the electron transition from the valance band to the conduction band, can be used to determine the nature and value of the optical band gap. The optical absorption study was used to determine the optical band gap of the nanoparticles, which is the most familiar and simplest method.

Table 1 – Structural, optical and electrical parameters of NiO:Fe thin film at different iron percentages

Percentage Fe (%)	Crystallite size (nm)	Strain ε (%)	Band gap energy (eV)	Conductivity 10^{-4} $(\Omega\ cm)^{-1}$
0	13.5	0.854	3.980	0.366
3	8.8	1.304	3.970	0.295
6	22.0	0.553	3.965	0.470
9	27.6	0.452	3.960	0.303
12	18.5	0.647	3.940	0.283
15	27.6	0.450	3.810	0.279
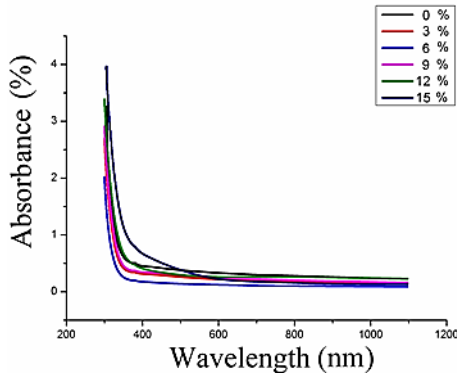
**Fig. 4** – Absorbance spectra of NiO samples for different percentage of Fe

The absorption coefficient (α) and the incident photon energy ($h\nu$) are related by the expression 2 [12]:

$$\left(\alpha h\upsilon\right) = C\left(h\upsilon - E_g\right)^n \qquad (2)$$

where α is the absorption coefficient, C is a constant, $h\nu$ is the photon energy, υ is the frequency of the incident radiation, h is the Planck's constant, exponent n is 0.5 for direct band allowed transition ($h\upsilon = 1239/\lambda(nm)$ (eV)) and E_g the band gap energy of the semiconductor.
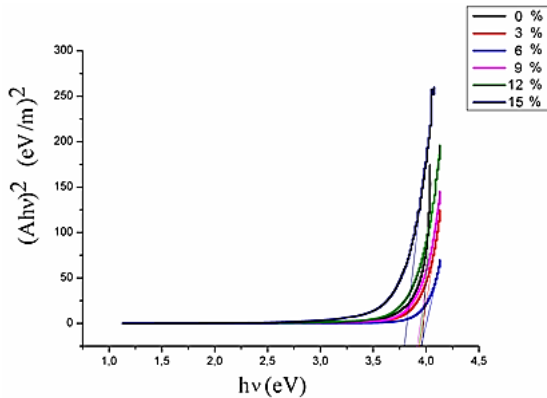
Fig. 5 – Plot of $(\alpha h\upsilon)^2$ versus incident photon energy ($h\nu$) of NiO:Fe nanoparticles for different percentage of Fe

As it was shown in (Fig. 5) a typical variation of $(\alpha h\upsilon)^2$ as a function of photon energy ($h\nu$) of NiO:Fe nanoparticles Eq. (2), used for deducing optical band gap E_g, The optical band gap values have been determined by extrapolating the linear portion of the curve to meet the energy axis ($h\nu$) [15]. The band gap values were given in Table 1.
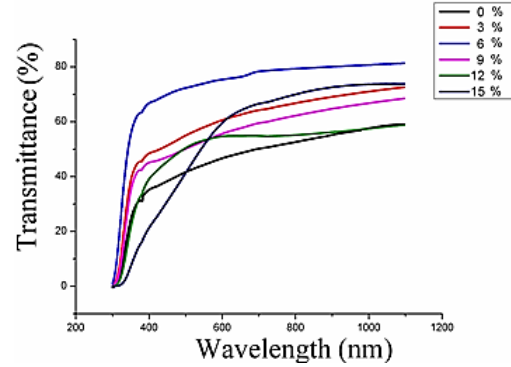
**Fig. 6** – Transmission spectra of NiO:Fe samples for different percentage of Fe

For a transmittance study (Fig. 6), the NiO:Fe layer showed very high transmittance of 80 % for 6 % iron concentration, averaged in the wavelength (λ) of 300-1100 nm. Suppression of light reflection at a surface is an important factor to absorb more photons in semiconductor materials. We obtained the reflectance profiles of NiO:Fe coated (Fig. 7). The averaged reflectance values (300-1100 nm) were significantly lower than 20 %. Moreover, NiO:Fe coating drives a substantially suppressed reflectance under 20 % in 500 nm $< \lambda <$ 1100 nm. This notifies that the NiO:Fe coating is an efficient design scheme to introduce the incident light into substrate.
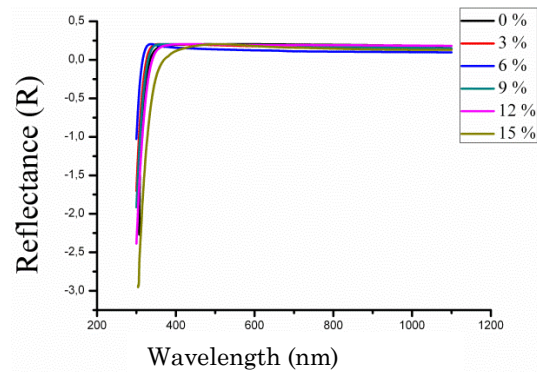
Fig. 7 – Reflectance profiles of NiO;Fe thin film for different percentage of Fe

3.3 Electrical Properties

The electrical properties of the NiO:Fe films are summarized in Table I. Fig. 8 shows the variation of the electrical conductivity σ of NiO:Fe thin films as a function as percentage of Fe. As can be seen, deposited films have good conductivity. The maximum recorded value was 0.470 10^{-4} $(\Omega\ cm)^{-1}$ for the NiO:Fe thin film depos-

ited using 6 % iron concentration. The increase of the electrical conductivity can be explained by the increase in the carrier concentration. Patil et al. [16] have reported that the increase of the electrical conductivity is due to the increase in activation energy with increasing film thickness. This was explained by difference in the experimental conditions of spraying solution, spray rate and cooling of the substrates during decomposition. However, with 0.20 mol L^{-1} precursor molarity, the crystal structure of the film is significantly improved and the grain size is increased, leading to a reduced concentration of structural defects such as dislocations and grain boundaries. Thus, the decrease of the concentration of crystal defects leads in the increase of free carrier concentration. The improvement of crystal quality reduces the carrier scattering from structural defects, leading to higher mobility.
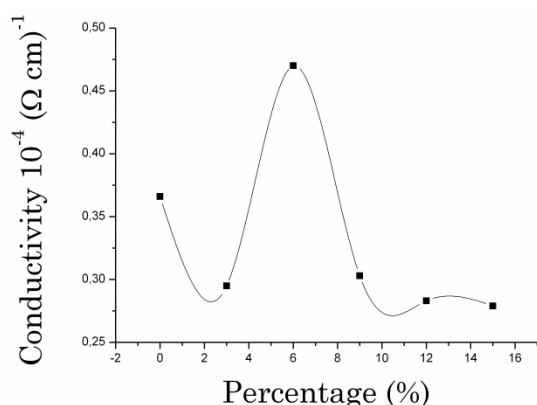
Fig. 8 – Variation of the electrical conductivity of NiO:Fe thin films as a function of the percentage of Fe

4. CONCLUSION

The spray pneumatic technique has been successfully employed to deposit NiO:Fe thin films with different iron concentrations on glass substrates. All the films showed cubic crystal structure with preferential orientation according to the direction (111). The maximum crystallite size was found (27.06 nm). We have observed an improvement in the films crystallinity at 0.10 mol L^{-1} precursor molarity where the peak at position 37.1° corresponding to the (111) plans is very sharp, the film obtain at this concentration has higher and sharper diffraction peak indicating an improvement in peak intensity compared to other films. The band gap value of NiO:Fe films was found from 3.810 eV to 3.980 eV. The high transmittance (80 %), low reflectance under 20 %, widened band gap and good conductivity ($0.470 \ 10^{-4} \ (\Omega \ cm)^{-1}$) obtained for NiO:Fe thin films make them promising candidate for optoelectronic devices as well as window layer in solar cell applications.

REFERENCES

1. M.A. Abbasi, Z.H. Ibupoto, A. Khan, O. Nur, M. Willander, *Mater. Lett.* **108**, 152 (2013).
2. M.D. Irwin, D.B. Buchholz, A.W. Hains, R.P.H. Chang, T.J. Marks, *Proc. National Academy Sci.* **105**, art. No 0711990105 (2008).
3. M. Ghougali, O. Belahssen, A. Chala, *J. Nano- Electron. Phys.* **8** No 4, 04059 (2016).
4. J. Kim, J.-H. Yun, Y.C. Park, W.A. Anderson, *Mater. Lett.* **75**, 99 (2012).
5. M.-J. Park, J.-Y. Jung, S.-M. Shin, J.-W. Song, Y.-H. Nam, D.-H. Kim, *Thin Solid Films* **599**, 54 (2016).
6. K.C. Wang, P.S. Shen, M.H. Li, S. Chen, M.W. Lin, P. Chen, *ACS Appl. Mater. Interf.* **6**, 11851 (2014).
7. J.H. Yun, J. Kim, Y.C. Park, S.J. Moon, W.A. Anderson, *Thin Solid Films* **547**, 17 (2013).
8. S. Ahn, A.H. Tuan, S. Kim, C. Park, C. Shin, Y.J. Lee, *Mater. Lett.* **132**, 332 (2014).
9. M. Ghougali, O. Belahssen, A. Chala, *J. Nano- Electron. Phys.* **9** No 3, 03043 (2017).
10. D. Zaouk, Y. Zaatar, R. Asmar, *Microelectron. J.* **37**, 11 (2006).
11. A.R. Balu, V.S. Nagarethinam, N. Arunkumar, M. Suganya, *J. Electron. Dev.* **13**, 739 (2012).
12. R. Sharma, A.D. Acharya, S.B. Shrivastava, M.M. Patidarc, M. Gangradec, T. Shripathic, V. Ganesan, *Optik* **127**, 4661 (2016).
13. J. Daniel Bayan, Daniel R. Gametin, *Prog. Inorgan. Chem.* **47** (2005).
14. B.D. Cullity, *Elements of X-ray Diffraction* (Addison-Wesley Publishing Co. Inc.: New York: 1976).
15. P.M. Ponnusamy, S. Agilan, N. Muthukumarasamy, T.S. Senthil, G. Rajesh, M.R. Venkatraman, D. Velauthapillai, *Mater. Character.* **114**, 166 (2016).
16. P.S. Patil, L.D. Kadam, *Appl. Surf. Sci.* **199**, 211 (2002).